Rate-Limiting Reaction of Dehydrogenative Dimerization of Ethanol to Ethyl Acetate and Hydrogen on Cu, Cu_2, and Cu_{13} Clusters: Size Dependence

Kang Sun,[†,‡,*] Zhipeng Wu,[‡,*] Ruitao Wu,[†] Yifei Chen,[‡] Minhua Zhang,[‡,**] and Lichang Wang[†,**]

[†]Department of Chemistry and Biochemistry, Southern Illinois University, Carbondale, Illinois 62901, United States;
[‡]Key Laboratory of Ministry of Education for Green Chemical Technology and Tianjin University-SINOPECR & D Center for Petrochemical Technology, Tianjin University,Tianjin 300072, China

Abstract

The reaction mechanisms of hydrogen and ethyl acetate formation from ethanol dehydrogenation in the presence of a single Cu atom, Cu_2, and Cu_{13} were studied using density functional theory (DFT) calculations. The rate-limiting step was found to be dependent on the Cu cluster size. The acetaldehyde prefers desorbing from Cu clusters due to its low adsorption energy on Cu, rather than dehydrogenating to acetyl. The vibrational frequencies of the system and temperature also affect the reaction mechanism. The HOMO-LUMO gap of the Cu_{13} cluster rarely altered by adsorption species while that of a single Cu and Cu_2 changed substantially when reactive species adsorbed on a single Cu atom or Cu_2 cluster. This work also illustrates that the reaction mechanisms are sensitive to the size of Cu clusters.

KEYWORDS: *copper cluster; ethanol; ethyl acetate; density functional theory, rate limiting step*

---

* These authors contributed equally to this work.
**Corresponding authors: lwang@chem.siu.edu (LW); mhzhang@tju.edu.cn (MZ)

1. Introduction

Ethyl acetate (EA) has been widely used as a solvent in the paints, coatings, adhesives and inks industries. Because of its low toxicity, it has also been employed as a solvent in many chemical processes to replace solvent containing aromatic compounds that generate serious damage to the environment and human beings. Three traditional processes for ethyl acetate synthesis are used in industry, including esterification of ethanol with acetic acid,[1] addition of ethylene to acetic acid,[2] and the Tishchenko reaction of acetaldehyde.[3] However, there are many problems associated with these processes, such as toxicity of acetaldehyde, facilities corrosion from acetic acid, or non-renewable feedstocks. Therefore, a novel process, ethanol acetate synthesis from ethanol dimerization, has become a promising process. It possesses several advantages, such as noncorrosive to the equipment, less toxic to the environment, only one ethanol feedstock, and renewable feedstock from bioethanol. Ethanol can be a product from the renewable sources, such as corn, cane and cassava.

Varieties of catalysts for this synthesis route have been reported previously. Cui et al.[4] reported that the ethanol conversion and the product selectivity were 88% and 48%, respectively, with MoS_2/C catalyst under optimum conditions. However, Cu-based catalysts are the most popular catalysts for this reaction. Iwasa et al.[5] reported the dehydrogenative dimerization of ethanol over several copper-based catalysts (Cu, Cu/SiO_2, Cu/ZrO_2, Cu/Al_2O_3, Cu/MgO, and Cu/ZnO).The selectivity of ethyl acetate markedly depended upon the supports part. The highest selectivity to ethyl acetate could reach 27.6% at 50% conversion of ethanol when using Cu/ZrO_2as catalyst, in which case a higher selectivity to the byproduct acetaldehyde was 57.3%. It also can be concluded that the dehydrogenation step occurs on the surface of metallic Cu from their work. Condensation reaction between ethanol and acetaldehyde occurs on the support of Cu/ZrO_2, whereas for the

Cu/SiO_2, it occurs on Cu surface.[5] However, Wang el at.[6] reported that for the Cu/ZrO_2catalyst, the highest conversion yield (70.9%) and selectivity (78.8%) to ethyl acetate were observed. Their results also indicated that metallic Cu phase acted as an active center for the dehydrogenation of ethanol. Inui el at.[7] reported that the maximum selectivity to ethyl acetate was 93% on the Cu-Zr-Al-O catalyst. This catalyst has already been industrially exploited. Colley et al.[8] reported another catalyst Cu/Cr_2O_3,with the highest selectivity of 95% for ethyl acetate reported now, has also been commercialized. In their TPR (temperature programmed reduction) studies, unsupported and Cr_2O_3supportedCucatalysts exhibit the same product spectrum. Therefore, Colley et al.[8] confirmed that Cu was the active component for this process. A reaction pathway was proposed based on their TD ethanol dosing experiments and TPR studies, as shown in the following schematic diagram.

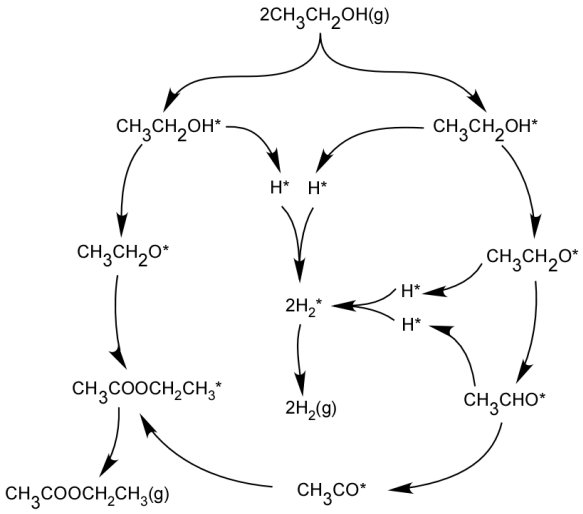

Scheme 1. A schematic diagram for ethyl acetate formation from ethanol dehydrogenation on the Cu catalyst, where the subscripts "*" and "g" refer to the adsorbed and gas phase species, respectively.

The reaction pathway involves the main possible species, reactant ethanol, intermediates such as ethoxy, acetaldehyde, and acetyl as well as product ethyl acetate. Firstly, the ethanol in gas

phase adsorbs on the Cu. Secondly, ethanol dehydrogenates to the ethoxy. Thirdly, the ethoxy dehydrogenates to the acetaldehyde. Fourthly, the acetaldehyde dehydrogenates to the acetyl. Then, the ehoxy and acetal species adsorbed on the Cu react to form adsorbed ethyl acetate molecule that migrates over the Cu to the Brönsted acid site on the Cr_2O_3, where it strongly adsorbed. The rate-determining step for the reaction is the desorption of the product ethyl acetate molecule from the Brönsted acid site.[8]

The decomposition of ethanol on Pt(111),[9,10] Rh(111),[11] Pd(111),[12] Pd(100),[13] $Rh/CeO_2(111)$,[14] $Ru/ZrO_2(111)$,[15,16]and $2Rh/\gamma\text{-}Al_2O_3(110)$[17]have been theoretically investigated using the density functional theory (DFT) calculation. The theoretical works relevant to dimerization of ethanol to ethyl acetate on pure Cu surfaces and alloys were also reported recently.[18-23] Due to the potential applications of ethanol fuel cells, many catalytic studies of ethanol oxidation were also been conducted recently on Ir[24-29] as well as other catalysts[30-58]

The study of nanosized metal clusters, such as Pt,[59-67] Au,[68-71] Pd,[72-79] Cu,[80-84] Ir,[85-87] and the alloys,[88-96] has been one of the most active research fields of chemistry, biology, and physics over the years due to their potential applications. Copper nanoparticles have potential applications in many areas including catalysis, data storage, medical diagnosis, optoelectronics, magneto-electronics, biochemistry and biosensing.[82,97-105] In order to understand the different properties of Cu nanoparticles and their catalytic activity, neutral and charged clusters have been studied using different theoretical and experimental approaches.[97,103] The synthesis of copper nanoparticles with controllable sizes, shapes, and surface properties is vital to exploring copper-based catalysis.[81-84,106-109]

The aim of this research is to investigate the synthesis of ethyl acetate from ethanol dimerization on small Cu_n (n=1, 2, 13) clusters. Based on the pathway proposed by Colley et al.,[8]

a series of DFT calculations were carried out on the adsorption of ethanol, ethoxy, acetaldehyde, acetyl, and ethyl acetate on small Cu clusters. The transition state (TS) was also obtained for each elementary step. The rate-limiting steps on different small Cu clusters were then determined and the size effect was investigated.

2. Computational Details

The DFT calculations were performed with the program package of DMol^3 in the Materials Studio of Accelrys, Inc.[110-112] The exchange and correlation energies were calculated using the Perdew-Burke-Ernzerhof (PBE) functional.[113,114] A double-numerical basis set with polarization functions (DNP) was used. Spin unrestricted DFT calculations were carried out in this work. The convergence criteria included threshold values of 2×10^{-5} Ha, 0.004 Ha/Å and 0.005 Å for energy, Max. force, and Max. displacement, respectively, while the self-consistent-field (SCF) density convergence of 1.0×10^{-5} Ha was employed. The same set of criteria was used in our previous studies of ethanol dehydrogenation and C-C bond cleavage on Cu surfaces.[18-23]

The decomposition of ethanol and the synthesis of ethyl acetate were first studied on small Cu_n clusters (n=1, 2). Then the Cu cluster was increased to around 0.5 nm size, Cu_{13}. All the adsorption states were relaxed. The vibrational analysis was done for all the Cu_n clusters and the adsorption complexes involved in the reaction pathways. Each minimum structure was characterized by the absence of imaginary frequencies.

The adsorption energies were calculated using the equation

$$\Delta E_{ad} = E_{adsorbate} + E_{Cu_n} - E_{adsorbate/Cu_n} \quad , \quad (1)$$

where $E_{adsorbate}$ is the total energy of the gas phase adsorbate molecule, E_{Cu_n} is the total energy of the Cu_n cluster, and $E_{adsorbate/Cu_n}$ is the total energy of the adsorbate on Cu_n. It is worth

mentioning that all the energies were after the zero point energy (ZPE) correction. By this definition, a positive ΔE_{ad} implies a stable adsorption.

For a dehydrogenation reaction, such as AH→A+ H, on Cu_n clusters, the reaction energy was calculated on the basis of the following formula:

$$\Delta E = E_{(A+H)/Cu_n} - E_{AH/Cu_n} \qquad (2)$$

Where $E_{(A+H)/Cu_n}$ is the total energy for the coadsorbed A and H on Cu_n clusters, and E_{AH/Cu_n} is the total energy of AH adsorbed on Cu_n.

Transition state (TS) searches were performed at the same theoretical level as those for the intermediates with the complete linear synchronous transit (LST)/ quadratic synchronous transit (QST) method.[110-112,115] In this method, the LST maximization was performed, followed by an energy minimization in directions conjugating to the reaction pathway to obtain an approximated TS. The approximated TS was then used to perform QST) maximization and then another conjugated gradient minimization was performed. The cycle was repeated until a stationary point was located. Then, the transition state optimization was executed in view of the structure from TS searching step. Each TS structure was characterized by a vibrational analysis with the presence of one imaginary frequency only. The activation barrier for an elementary step is defined to be the difference between the energies of the TS and the initial state (IS), which is the adsorbed reactant unless noted otherwise:

$$\Delta E_a = E_{TS} - E_{IS} \ . \qquad (3)$$

The harmonic transition state theory, expressed as followed,[116-118]

$$k = \frac{\prod v_i}{\prod v_i^{\neq}} e^{-\frac{Ea}{k_B T}} \qquad (4)$$

was used to calculate the rate constant k for each elementary step involved in the reaction pathway. In eq.(4), v_i and $v_i^{\neq}$ are the frequencies of reactant and transition state, respectively. E_a is the reaction barrier. k_B and T denote the Boltzmann constant and temperature, respectively. We note that no quantum effect[119] or high temperature effect[120] are considered in the kinetics calculations.

3. Results and Discussion

In this part, all the species included in the reaction were optimized. The most stable optimum isomers for each adsorbate were listed in Table 1 and 2. The configurations of initial state (IS), transition state (TS) and final state (FS) for each elementary step, the relationships between the rate constant *k* and the temperature for each elementary step were shown in Table 1-2 and Figure 1-7. The correlation between the activation energy and the HOMO-LUMO gap of Cu clusters was investigated. In addition, the rate limiting steps on Cu_n (n=1, 2, 13) clusters were also discussed.

3.1 Elementary Steps on a Single Cu Atom

On a single cupper atom, five elementary steps were studied using the DFT method. The most stable structures for ethanol, ethoxy, acetaldehyde, ethoxy and acetyl co-adsorption, and two H atoms co-adsorption were selected to be the initial states (IS1 to IS5), which were shown in Table 1 and Figure 1. Owing to the closed-shell electronic configuration of ethanol and acetaldehyde, there exist weak interactions between these two species and a single Cu atom with the adsorption energies of 0.26 eV and 0.25 eV, respectively. By contrast, ethoxy adsorbed strongly on a Cu atom with a world-apart adsorption energy of 2.45 eV, since the O atom of ethoxy is highly unsaturated. Figure 1 illustrates that the highest activation barrier (1.04 eV) was obtained on the dehydrogenation of ethoxy, followed by a slightly lower activation barrier of 1.02 eV on the dehydrogenation of ethanol, indicating that these two elementary steps might be the rate limiting steps of athyl acetate production from ethanol dimerization on single Cu atom. However, it was

not the exact rate-determined step in high temperature condition since the reaction rate constant varies with temperature, which will be discussed in the later section.

Regarding to the dehydrogenation of acetaldehyde, the activation energy for this step was much higher than the adsorption energy of the reactant on a single Cu atom (0.64 eV > 0.25 eV), indicating that acetaldehyde was more likely to desorb from a single Cu atom than to dehydrogenate to acetyl, which agreed with the experimental results.[5] We note that defects may play important roles as well.[121,122] Thus the result can infer that a single Cu atom is not active enough to catalyze ethanol dimerization since it cannot activate ethanol easily. In addition, all of the three dehydrogenation steps from ethanol and the formation of hydrogen molecular were exothermic reactions with the reaction energies of -0.13 eV, -0.41 eV, -0.15 eV and -0.23 eV, respectively. However, the formation of ethyl acetate was an endothermic one (0.28 eV). It was very intriguing that almost all of the C2 species were bonded with single Cu atom via O atom except for acetyl, which might be attributed to the high saturation of tetravalent C atom with H atoms on them. The products chemi-adsorbed weakly on single Cu atom with the adsorption energies of 0.16 eV and 0.07 eV for ethyl acetate and hydrogen molecular, respectively, corresponding to the nearest Cu-O bond and Cu-H bond distances of 2.797 Å and 2.383 Å, respectively, which were really weak interactions. Finally, we note that in the case of single atom catalysis,[123,124] the metal atom is often accompanied with ligands[125-128] or substrates.[129,130]

3.2 Elementary Steps on the Cu_2 Cluster

Similarly, identical elementary steps were calculated on Cu_2 cluster. The most stable configurations of reactants and products were selected as the initial states (IS1 to IS5) and the final states (FS1 to FS5), including some co-adsorptions shown in Figure 2. Figure 2 demonstrated that it was difficult to dehydrogenate acetaldehyde and to form hydrogen molecular on Cu_2 cluster

with the reaction barriers of 1.16 eV and 1.19 eV, respectively. But it was easy to dehydrogenate ethoxy (0.52 eV) and generate athyl acetate (0.48 eV). The dehydrogenation of ethanol on Cu_2 cluster was not smooth with the high activation barriers of the first (1.02 eV) and the third (1.16 eV) dehydrogenation steps, leading to a poor catalytic performance of Cu_2 cluster, just like single Cu atom.

Analogous to single Cu atom, the following similar phenomena occurred again on Cu_2 cluster. Ethanol and acetaldehyde adsorbed weakly on Cu_2 cluster with the adsorption energies of 0.62 eV and 0.64 eV, by contrast, ethoxy adsorbed strongly on Cu_2 cluster (ΔE_{ad} =1.76 eV). The C2 species bonded with Cu_2 cluster via O atoms except for acetyl. Besides, athyl acetate (ΔE_{ad} =0.47 eV) and hydrogen molecular (ΔE_{ad} =0.26 eV) chemi-adsorbed weakly on Cu_2 cluster. Acetaldehyde desorption was easier than dehydrogenation to acetyl (1.16 eV > 0.64 eV) on Cu_2 cluster. These similar natures resulted from the properties of the reactants and intermediates, which scarcely affected by the catalysts.

In Figure 2(e), two hydrogen atoms on Cu_2 cluster formed structure IS5. One H adsorbed on a top site, while another adsorbed on a bridge site. The TS5 structure on Cu_2 illustrated that one of the Cu-H bonds should break firstly to form hydrogen molecular, while FS5 configuration showed that the hydrogen molecular was likely to adsorb on a atop site on Cu_2. Dehydrogenation of ethanol, i.e. O-containing species, may also be very different from that of alkanes[131-134] where the C-C bond strength is different.[132]

3.3 Elementary Steps on the Cu_{13} Cluster

In these cases, as illustrated in Table 1 and Figure 3, five corresponding steps were carried out on Cu_{13} cluster, whose diameter rose to about 0.5 nm. Higher catalytic performance was observed on Cu_{13} cluster with lower reaction barriers. In comparison, lower reaction barriers 0.75

eV, 0.54 eV and 0.63 eV, respectively, were obtained for three dehydrogenation steps from ethanol to acetyl on Cu_{13} cluster, implying that it became easier for ethanol activation.

Table 1 and Figure 1(b) showed that the activation energy for reverse reaction from acetaldehyde to ethoxy on Cu_1 was 1.45 eV, which was much higher than the desorption energy (0.25 eV) for acetaldehyde on Cu_1. Similarly, Cu_2 and Cu_{13} clusters met with the same situation. As a result of this, once the acetaldehyde produced, it preferred to desorb to the gas state than to decompose. In this sense, this whole reaction prefers to produce acetaldehyde than further dehydrogenates to produce ethyl acetate, which led to a lower selectivity of ethyl acetate.

With the lowest reaction barrier of 0.39 eV, it was prone to form ethyl acetate when ethanol was activated to acetyl. The formation of hydrogen molecular was the most difficult step with the highest activation barrier of 0.88 eV, which might be the rate limiting step on Cu_{13} cluster. However, it was still the lowest reaction barrier on Cu_n (n=1, 2, 13)clusters. By the same reason, similar properties of the reactants and intermediates occurred again on Cu_{13} cluster.

Figure 3(a) showed that the O-H bond orientation was parallel to the Cu-O direction in IS1, meanwhile, the steady ethoxy and atomic H co-adsorption state on the Cu_{13} clusters was shown in FS1. The atomic H was also likely to adsorb on the bridge site of Cu_{13}. The activation energy barrier for this case was the lowest 0.75 eV. It maybe because the Cu_{13} cluster acts more like a surface Cu. Figure 1(b), 2(b) and 3(b) showed that the FS2 was a structure of acetaldehyde and atomic H co-adsorbed on Cu_n (n=1, 2, 13) clusters. The Cu atom both bonded with the carbon and oxygen in acetaldehyde on single Cu and Cu_2 clusters, however, only the oxygen in acetaldehyde adsorbed on atop site via Cu-O bond on Cu_{13} clusters. The possible reason maybe the steric hindrance effect between acetaldehyde and Cu_{13} clusters. In Figure 2(d) and 3(d), the α-C in the acetyl adsorbed on the bridge site on Cu_2 cluster while both of the ethoxy and acetyl adsorbed at

atop site on Cu_{13}, indicating that larger size brought more adsorption sites and more activation sites which brought down the reaction barrier, in the case of such a big size molecular. Figure 3(e) illustrated that the two hydrogen atoms both adsorbed on the bridge site in structure IS5. When the hydrogen molecular formed, it was also likely adsorbing on a top site of Cu_{13} as shown in structure FS5.

3.4 Correlation between the Activation Energy and the HOMO-LUMO Gap of Cu Clusters

In order to find out the dominated factor which controls the catalytic activity of ethyl acetate synthesis from ethanol dehydrogenation on small Cu_n(n=1,2,13) clusters, we calculated the HOMO-LUMO gap. The HOMO-LUMO gaps of the systems with and without adsorbed species were shown in Table 2.

On Cu_1 and Cu_2 clusters, the HOMO-LUMO gap of the system changed only slightly after the ethanol and acetaldehyde adsorbed because of the weak adsorption. Nevertheless, ethoxy adsorbed strongly on Cu_n(n = 1, 2) clusters, thus it influenced the electron orbital distribution of the system which makes the HOMO-LUMO gap change a lot after it adsorbed on Cu_n(n = 1, 2) clusters. As for Cu_{13} cluster, the adsorption species have almost no effect on the HOMO-LUMO gap. These results suggested that the HOMO-LUMO gap of larger size Cu cluster are not influenced by adsorption species.

A small HOMO-LUMO gap corresponds to a high chemical reactivity and low reaction activation energy. The relationship between the reaction activation energy and the HOMO-LUMO gap of the system for dehydrogenation steps was fitted as shown in Figure 4.For ethanol and acetaldehyde dehydrogenation as shown in Figure 4 (a),(c),(d)and(f), there was a good linear relationship between the activation energy and the HOMO-LUMO gap. This is because the HOMO-LUMO gap of ethanol and acetaldehyde before and after adsorbed on Cu clusters changed

a little as mentioned above. For ethoxy dehydrogenation, it showed a terrible linear relationship between the activation energy and the HOMO-LUMO gap of Cu clusters without ethoxy adsorbed. However, as shown in Figure 4(e), after ethoxy adsorbed on Cu clusters, the linear relationship of the reaction activation energy and the system's HOMO-LUMO gap became better. This is due to the strong adsorption of ethoxy on Cu clusters altered the HOMO-LUMO gap of the bare cluster. A good linear relationship implied that the catalytic reactivity of Cu clusters was dominated by HOMO-LUMO gap of the system with adsorbed species.

To verify this conclusion, the reverse reactions of the dehydrogenation of ethanol, ethoxy and acetaldehyde were also investigated. The linear relationship between the reaction activation energy of hydrogenation and the HOMO-LUMO gap of the system was shown in Figure 5.The nice linear correlation verified that the activation energy on Cu clusters was decided by the system's HOMO-LUMO gap after each reaction species.

The adsorption of ethoxy could rearrange the electron orbital distributions and change the HOMO-LUMO gap of Cu_1 and Cu_2 clusters, which resulted in the fluctuation of the catalytic activation energy for elementary steps. However, the electron orbital distributions of larger size Cu_{13} cluster was slightly impacted by adsorbates. Therefore, in order to avoid unstable catalytic activation with different adsorbed molecules, larger clusters should be chosen. Here, we showed that one can investigate the influence of adsorption species on the HOMO-LUMO gap of different sizes of metal clusters, then choose moderate size clusters whose electron orbitals would not be easily changed by adsorption species for robust catalysis.

3.5 Rate Limiting Step: Cluster Size Dependence

Figure 6 illustrated the variation of the forward reaction constant k with the changing temperature of each elementary step. Figure 6(a) showed that ethanol dehydrogenation to ethoxy

on Cu_{13} predicted the largest forward reaction constant while on a single Cu atom and Cu_2 revealed the similar lowest one. In Figure 6(b), the forward reaction constant of ethoxy dehydrogenation to acetaldehyde on Cu_2 was a little higher than that on Cu_{13}, and all of them were much higher than that on Cu_1. Figure 6(c) illustrated an adjacent line of Cu_1 and Cu_{13}, meanwhile, they were extremely higher than Cu_2. Figure 6(d) indicated that the catalytic activity of Cu clusters for the synthesis of ethyl acetate from ethoxy and acetyl was in this order: Cu_{13}, Cu_2 and Cu_1, corresponding to increasing activation barrier for Cu_{13} (0.39 eV), Cu_2 (0.48 eV) and Cu_1 (0.86 eV) as shown in Figure 1-3. In this sense, lower activation barrier signified higher catalytic activation. Figure 6 (e) showed that the formation of hydrogen on Cu_{13} predicted the largest forward reaction constant while on Cu_2 revealed the lowest one.

Comparing with Figure 6(b) and (d), single Cu atom revealed the lowest catalytic activity. It might be due to the reactant of ethoxy dehydrogenation to acetaldehyde and the formation of ethyl acetate from ethoxy and acetyl were unsaturated coordinate. Ethoxy adsorbed on Cu clusters by Cu-O bond, so single Cu atom had no more Cu atoms for chemical adsorption while Cu_2 and Cu_{13} clusters predicted higher activity with spare Cu atoms. As for Figure 6 (a), (c) and (e), Cu_2 cluster showed an obvious lower catalytic activity than Cu_1 and Cu_{13}. A hypothesis was that Cu had odd-even effect like Au and Ag. The electrons in two Cu atoms of even number Cu_2 cluster were internally saturated while odd number Cu_1 and Cu_{13} cluster had single electron which led to a higher catalytic activity. To summarize, Cu_{13} cluster manifested higher catalytic activity comparing with Cu_1 and Cu_2 clusters.

Figure 7 implied the correlation between the rate constant and the temperature of each elementary step for ethyl acetate synthesis from ethanol dehydrogenation on small Cu_n (n=1,2,13) clusters. As shown in Figure 7(a), ethanol dehydrogenation to ethoxy and ethoxy dehydrogenation

to acetaldehyde were the rate-limiting steps on Cu_1 when T <524 K, but the rate-limiting step on Cu_1 became the formation of ethyl acetate from ethoxy and acetyl when T > 524 K. As a matter of fact, the temperature of the formation of ethyl acetate from ethanol dehydrogenation in industry was about 493 K, so under this temperature, the rate-limiting steps on Cu_1 were ethanol dehydrogenation to ethoxy and ethoxy dehydrogenation to acetaldehyde. Figure 7(b) and Figure 7(c) showed that the rate-limiting steps on Cu_2 and Cu_{13} were both the formation of hydrogen molecules. These comparisons illustrated that the reaction mechanism of ethyl acetate synthesis from ethanol dehydrogenation really depended on the different sizes of small Cu clusters.

4. Conclusions

The reaction mechanisms of ethyl acetate synthesis from ethanol dehydrogenation on small Cu_n（n=1, 2, 13）clusters have been investigated using the DFT method. Ethanol dehydrogenation to ethoxy and ethoxy dehydrogenation to acetaldehyde were the rate-limiting steps on Cu_1 when T <524 K, but the rate-limiting step on Cu_1 became the formation of ethyl acetate from ethoxy and acetyl when T > 524 K. The rate-limiting steps on Cu_2 and on Cu_{13} were both the formation of hydrogen molecules. Based on the DFT results, it can also be concluded that the exothermic and endothermic reactions were not always equal to tending to get the product, which was with lower system energy. The vibrational frequencies of the system and temperature also affected the reaction mechanism. Owing to its low adsorption energy on Cu, acetaldehyde preferred desorbing from small Cu clusters rather than dehydrogenation to the acetyl. After the strong adsorption species adsorbed on single Cu atom and Cu_2 cluster, the electron orbital distribution changed easily, corresponding to the change of the HOMO-LUMO gap of the system. However, the HOMO-LUMO gap of larger size Cu_{13} cluster was rarely influenced by adsorption species. As for each elementary steps of the formation of ethyl acetate from ethanol

dehydrogenation, the dominant influence factor of the activation energy of ethanol dehydrogenation on Cu clusters was the HOMO-LUMO gap of the system after reactive species adsorbed on Cu clusters. In addition, this work illustrated that the reaction mechanism can depend on the size of Cu clusters. To understand the performance of Cu catalyst and the size effect, further work on Cu_{55} will be interesting.

▪ ASSOCIATED CONTENT

Supporting Information

The coordinates of the reported systems. This material is available free of charge via the Internet at .

▪ AUTHOR INFORMATION

Corresponding Authors

L. Wang: lwang@chem.siu.edu and M. Zhang: mhzhang@tju.edu.cn

Notes

The authors declare no competing financial interest.

▪ ACKNOWLEDGMENTS

K. Sun acknowledges the support from the China Scholarship Council for his stay in Carbondale where most of the work described here was carried out.

▪ REFERENCES

(1) McMurry, J. *Organic Chemistry, 5th Edition*; Brooks/Cole, 2000.
(2) Gregory, R.; Smith, D. J. H.; Westlake, D. J. *Clay Miner* **1983**, *18*, 431.
(3) Ogata, Y.; Kawasaki, A. *Tetrahedron* **1969**, *26*, 929.
(4) Cui, N.; Liu, C.; Jiang, H.; Zhang, M. *Chem. Ind. Eng.* **2006**, *23*.
(5) Iwasa, N.; Takezawa, N. *Bull. Chem. Soc. Jpn.* **1991**, *64*, 2619.
(6) Wang, L. X.; Zhu, W. C.; Zheng, D. F.; Yu, X.; Cui, J.; Jia, M. J.; Zhang, W. X.; Wang, Z. L. *React. Kinet. Mech. Catal.* **2010**, *101*, 365.
(7) Inui, K.; Kurabayashi, T.; Sato, S. *J. Catal.* **2002**, *212*, 207.
(8) Colley, S. W.; Tabatabaei, J.; Waugh, K. C.; Wood, M. A. *J. Catal.* **2005**, *236*, 21.

(9) Wang, H. F.; Liu, Z. P. *J. Phys. Chem. C* **2007**, *111*, 12157.
(10) Wang, H. F.; Liu, Z. P. *J. Am. Chem. Soc.* **2008**, *130*, 10996.
(11) Choi, Y.; Liu, P. *J. Am. Chem. Soc.* **2009**, *131*, 13054.
(12) Li, M.; Guo, W. Y.; Jiang, R. B.; Zhao, L. M.; Shan, H. H. *Langmuir* **2010**, *26*, 1879.
(13) Wang, E. D.; Xu, J. B.; Zhao, T. S. *J. Phys. Chem. C* **2010**, *114*, 10489.
(14) Chen, H. L.; Liu, S. H.; Ho, J. J. *J. Phys. Chem. B* **2006**, *110*, 14816.
(15) Chen, Y. W.; Ho, J. J. *J. Phys. Chem. C* **2009**, *113*, 6132.
(16) Chen, Y. W.; Wu, S. Y.; Ho, J. J. *Chem. Phys. Lett.* **2011**, *501*, 315.
(17) Wu, S. Y.; Lia, Y. R.; Ho, J. J.; Hsieh, H. M. *J. Phys. Chem. C* **2009**, *113*, 16181.
(18) Sun, K.; Zhang, M.; Wang, L. *Chem. Phys. Lett.* **2013**, *585*, 89.
(19) Xu, H.; Miao, B.; Zhang, M.; Chen, Y.; Wang, L. *Phys. Chem. Chem. Phys.* **2017**, *19*, 26210.
(20) Wu, Z.; Zhang, M.; Jiang, H.; Zhong, C.-J.; Chen, Y.; Wang, L. *Phys. Chem. Chem. Phys.* **2017**, *19*, 15444.
(21) Wu, R.; Sun, K.; Chen, Y.; Zhang, M.; Wang, L. *Surf. Sci.* **2021**, *703*, 121742.
(22) Wu, R.; Wang, L. *Chem. Phys. Lett.* **2017**, *678*, 196.
(23) Wu, R.; Wang, L. *Comput. Mater. Sci.* **2021**, *196*, 110514.
(24) Wu, R.; Wang, L. *ChemPhysChem* **2022**, e202200132.
(25) Wu, R.; Wang, L. *Chem. Phys. Impact* **2021**, *3*, 100040.
(26) Miao, B.; Wu, Z.; Xu, H.; Zhang, M.; Chen, Y.; Wang, L. *Chem. Phys. Lett.* **2017**, *688*, 92.
(27) Wu, R.; Wang, L. *J. Phys. Chem. C* **2020**, *124*, 26953.
(28) Wu, R.; Wiegand, K. R.; Wang, L. *J. Chem. Phys.* **2021**, *154*, 054705.
(29) Matsuda, S.; Masuda, S.; Takano, S.; Ichikuni, N.; Tsukuda, T. *ACS Catal.* **2021**, *11*, 10502.
(30) Wu, R.; Wang, L. *J. Phys. Chem. C* **2022**, *126*, 21650.
(31) Wu, R.; Wang, L. *Phys. Chem. Chem. Phys.* **2023**, *25*, 2190.
(32) Gebre, S. H.; Sendeku, M. G. *Journal of Energy Chemistry* **2022**, *65*, 329.
(33) Zhao, G. L.; Fang, C. H.; Hu, J. W.; Zhang, D. L. *ChemPlusChem* **2021**, *86*, 574.
(34) Xiao, F.; Wang, Y.-C.; Wu, Z.-P.; Chen, G.; Yang, F.; Zhu, S.; Siddharth, K.; Kong, Z.; Lu, A.; Li, J.-C.; Zhong, C.-J.; Zhou, Z.-Y.; Shao, M. *Adv. Mater.* **2021**, 2006292.
(35) Rizo, R.; Bergmann, A.; Timoshenko, J.; Scholten, F.; Rettenmaier, C.; Jeon, H. S.; Chen, Y.-T.; Yoon, A.; Bagger, A.; Rossmeisl, J.; Cuenya, B. R. *J. Catal.* **2021**, *393*, 247.
(36) Rizo, R.; Perez-Rodriguez, S.; Garcia, G. *ChemElectroChem* **2019**, *6*, 4725.
(37) Nosheen, F.; Anwar, T.; Siddique, A.; Hussain, N. *Frontiers in Chemistry* **2019**, *7*.
(38) Wang, Y.; Zou, S.; Cai, W.-B. *Catalysts* **2015**, *5*, 1507.
(39) Antolini, E. *RSC Adv.* **2016**, *6*, 3307.
(40) Chen, A.; Ostrom, C. *Chem. Rev.* **2015**, *115*, 11999.
(41) Miao, B.; Wu, Z.; Zhang, M.; Chen, Y.; Wang, L. *J. Phys. Chem. C* **2018**, *122*, 22448.
(42) Miao, B.; Wu, Z.-P.; Xu, H.; Zhang, M.; Chen, Y.; Wang, L. *Comput. Mater. Sci.* **2019**, *156*, 175.
(43) Lei, Y.; Liu, B.; Lu, J.; Lobo-Lapidus, R. J.; Wu, T.; Feng, H.; Xia, X.; Mane, A. U.; Libera, J. A.; Greeley, J. P.; Miller, J. T.; Elam, J. W. *Chem. Mater.* **2012**, *24*, 3525.
(44) Cai, J. D.; Huang, Y. Y.; Guo, Y. L. *Appl. Catal. B-Environ.* **2014**, *150*, 230.
(45) del Rosario, J. A. D.; Ocon, J. D.; Jeon, H.; Yi, Y.; Lee, J. K.; Lee, J. *J. Phys. Chem. C* **2014**, *118*, 22473−22478.

(46) Du, W.; Yang, G.; Wong, E.; Deskins, N. A.; Frenkel, A. I.; Su, D.; Teng, X. *J. Am. Chem. Soc.* **2014**, *136*, 10862.
(47) Xu, B. J.; Madix, R. J.; Friend, C. M. *Acc. Chem. Res.* **2014**, *47*, 761.
(48) Yang, Y.-Y.; Ren, J.; Li, Q.-X.; Zhou, Z.-Y.; Sun, S.-G.; Cai, W.-B. *ACS Catal.* **2014**, *4*, 798.
(49) Gomez, J. C. C.; Moliner, R.; Lazaro, M. J. *Catalysts* **2016**, *6*, 130.
(50) Monyoncho, E. A.; Steinmann, S. N.; Michel, C.; Baranova, E. A.; Woo, T. K.; Sautet, P. *ACS Catal.* **2016**, *6*, 4894.
(51) von Weber, A.; Anderson, S. L. *Acc. Chem. Res.* **2016**, *49*, 2632.
(52) Wang, J.; Li, B.; Yersak, T.; Yang, D. J.; Xiao, Q. F.; Zhang, J. L.; Zhang, C. *J. Mater. Chem. A* **2016**, *4*, 11559.
(53) Wang, W.; Lv, F.; Lei, B.; Wan, S.; Luo, M. C.; Guo, S. J. *Adv. Mater.* **2016**, *28*, 10117.
(54) Du, Y. L.; Wu, X.; Cheng, Q.; Huang, Y. L.; Huang, W. *Catalysts* **2017**, *7*.
(55) Sulaiman, J. E.; Zhu, S.; Xing, Z.; Chang, Q.; Shao, M. *ACS Catal.* **2017**, *7*, 5134.
(56) Wen, C.; Wei, Y.; Tang, D.; Sa, B.; Zhang, T.; Chen, C. *Sci. Rep.* **2017**, *7*, 4907.
(57) Liu, Y.; Wei, M.; Raciti, D.; Wang, Y.; Hu, P.; Park, J. H.; Barclay, M.; Wang, C. *ACS Catal.* **2018**, *8*, 10931.
(58) Bai, J.; Liu, D. Y.; Yang, J.; Chen, Y. *ChemSusChem* **2019**, *12*, 2117.
(59) Xiao, L.; Wang, L. *J. Phys. Chem. A* **2004**, *108*, 8605.
(60) Sun, S.; Wu, X.; Huang, Z.; Shen, H.; Zhao, H.; Jing, G. *Chem. Eng. J.* **2022**, *435*, 135035.
(61) Nair, A. S.; Anoop, A.; Ahuja, R.; Pathak, B. *J. Phys. Chem. C* **2022**, *126*, 1345.
(62) Taleblou, M.; Camellone, M. F.; Fabris, S.; Piccinin, S. *J. Phys. Chem. C* **2022**, *126*, 10880.
(63) Sumer, A.; Jellinek, J. *J. Chem. Phys.* **2022**, *157*, 034301.
(64) Bumüller, D.; Yohannes, A. G.; Kohaut, S.; Kondov, I.; Kappes, M. M.; Fink, K.; Schooss, D. *J. Phys. Chem. A* **2022**, *126*, 3502.
(65) Duan, S. B.; Du, Z.; Fan, H. S.; Wang, R. M. *Nanomater.* **2018**, *8*, 949.
(66) Xu, H.; Shang, H. Y.; Wang, C.; Du, Y. K. *Adv.Func.Mater.* **2020**, *30*.
(67) Huang, L.; Zaman, S.; Wang, Z. T.; Niu, H. T.; You, B.; Xia, B. Y. *Acta Physico-Chimica Sinica* **2021**, *37*, 2009035.
(68) Xiao, L.; Tollberg, B.; Hu, X.; Wang, L. *J. Chem. Phys.* **2006**, *124*, 114309.
(69) Piotrowski, M. J.; Orenha, R. P.; Parreira, R. L. T.; Guedes-Sobrinho, D. *J. Comput. Chem.* **2022**, *43*, 230.
(70) Iqbal, T.; Azam, A.; Majid, A.; Zafar, M.; Shafiq, M.; Ullah, S.; Hussien, M. *Opt. Quantum Electronics* **2022**, *54*, 74.
(71) Pakrieva, E.; Kolobova, E.; Kotolevich, Y.; Pascual, L.; Carabineiro, S. A. C.; Kharlanov, A. N.; Pichugina, D.; Nikitina, N.; German, D.; Partida, T. A. Z.; Vazquez, H. J. T.; Farías, M. H.; Bogdanchikova, N.; Corberán, V. C.; Pestryakov, A. *Nanomater.* **2020**, *10*, 880.
(72) Zhang, W.; Ge, Q.; Wang, L. *J. Chem. Phys.* **2003**, *118*, 5793.
(73) Gracia-Espino, E.; Hu, G.; Shchukarev, A.; Wågberg, T. *J. Am. Chem. Soc.* **2014**, *136*, 6626.
(74) Salabat, A.; Mirhoseini, F.; Mahdieh, M.; Saydi, H. *New. J. Chem.* **2015**, *39*, 4109.
(75) Yu, N.-F.; Tian, N.; Zhou, Z.-Y.; Sheng, T.; Lin, W.-F.; Ye, J.-Y.; Liu, S.; Ma, H.-B.; Sun, S.-G. *ACS Catal.* **2019**, *9*, 3144.
(76) Essoumhi, A.; El Kazzouli, S.; Bousmina, M. *J. Nanosci. Nanotechnol.* **2014**, *14*, 2012.

(77) Saldan, I.; Semenyuk, Y.; Marchuk, I.; Reshetnyak, O. *J. Mater. Sci.* **2015**, *50*, 2337.
(78) Iqbal, M.; Kaneti, Y. V.; Kim, J.; Yuliarto, B.; Kang, Y. M.; Bando, Y.; Sugahara, Y.; Yamauchi, Y. *Small* **2019**, *15*.
(79) Kumar, A.; Mohammadi, M. M.; Swihart, M. T. *Nanoscale* **2019**, *11*, 19058.
(80) Love-Nkansah, C. B.; Sun, K.; Zhong, C.-J.; Averkiev, B. B.; Truhlar, D. G.; Wang, L. *ChemRxiv* **2022**, *10.26434/chemrxiv-2022-78683*.
(81) Niu, Y.; Crooks, R. *Chem. Matter* **2003**, *15*, 3463.
(82) Yang, Y. X.; Evans, J.; Rodriguez, J. A.; White, M. G.; Liu, P. *Phys. Chem. Chem. Phys.* **2010**, *12*, 9909.
(83) Hoover, N.; Auten, B.; Chandler, B. D. *J. Phys. Chem. B.* **2006**, *110*, 8606.
(84) Mott, D.; Galkowski, J.; Wang, L.; Luo, J.; Zhong, C.-J. *Langmuir* **2007**, *23*, 5740.
(85) Lu, J.; Aydin, C.; Browning, N. D.; Wang, L.; Gates, B. C. *Catal. Lett.* **2012**, *142*, 1445.
(86) Ciborowski, S. M.; Buszek, R.; Liu, G.; Blankenhorn, M.; Zhu, Z.; Marshall, M. A.; Harris, R. M.; Chiba, T.; Collins, E. L.; Marquez, S.; Boatz, J. A.; Chambreau, S. D.; Vaghjiani, G. L.; Bowen, K. H. *J. Phys. Chem. A* **2021**, *125*, 5922.
(87) Poerwoprajitno, A. R.; Gloag, L.; Cheong, S.; Gooding, J. J.; Tilley, R. D. *Nanoscale* **2019**, *11*, 18995.
(88) Wanjala, B.; Lou, J.; Loukrakpam, R.; Mott, D.; Njoki, P.; Fang, B.; Engelhard, M.; Naslund, H. R.; Wu, J. K.; Wang, L.; Malis, O.; Zhong, C. J. *Chem. Mater.* **2010**, *22*, 4282.
(89) Wang, L.; Ore, R. M.; Jayamaha, P. K.; Wu, Z.-P.; Zhong, C.-J. *Faraday Discuss.* **2022**, DOI: 10.1039/d2fd00101b.
(90) Wu, X.; Wang, G.-Y.; Du, R.-B.; Tang, S. *Chem. Phys.* **2020**, *534*, 110751.
(91) Schulte, E.; Santos, E.; Quaino, P. *Surf. Sci.* **2020**, *697*, 121605.
(92) Zanti, G.; Peeters, D. *J. Phys. Chem. A* **2010**, *114*, 10345.
(93) Kattel, S.; Chen, J. G.; Liu, P. *Catal. Sci. Technol.* **2018**, *8*, 3748.
(94) Sial, M.; Din, M. A. U.; Wang, X. *Chem. Soc. Rev.* **2018**, *47*, 6175.
(95) Zhang, B. W.; Yang, H. L.; Wang, Y. X.; Dou, S. X.; Liu, H. K. *Adv. Energy Mater.* **2018**, *8*, 1703597.
(96) Huo, D.; Kim, M. J.; Lyu, Z.; Shi, Y.; Wiley, B. J.; Xia, Y. *Chem. Rev.* **2019**, *119*, 8972.
(97) Glaspell, g.; Abselseyed, V.; Saoud, K. M.; S., E.-S. M. *Pure and Appl. Chem.* **2006**, *78*, 1667.
(98) Kudo, S.; Maki, T.; Miura, K.; Mae, K. *Carbon* **2010**, *48*, 1186.
(99) Manceau, A.; Matynia, A. *Geochim. Cosmochim. Acta* **2010**, *74*, 2556.
(100) Gomez-Gualdron, D. A.; Zhao, J.; Balbuena, P. B. *J. Chem. Phys.* **2011**, *134*, 11.
(101) Li, M. Y.; Huang, Y. S.; Jeng, U. S.; Hsu, I. J.; Wu, Y. S.; Lai, Y. H.; Su, C. H.; Lee, J. F.; Wang, Y.; Chang, C. C. *Biophys. J.* **2009**, *97*, 609.
(102) M Scarselli, P Castrucci, L Camilli, S Del Gobbo, S Casciardi, F Tombolini, E Gatto, M Venanzi and M De Crescenzi *Nanotechnology* **2011**, *22*.
(103) Matsui, I. *Japanese J. Appl. Phys. Part 1* **2006**, *48*, 8302.
(104) Kang, J.; Zhang, X. X. *Prog. Chem.* **2006**, *18*, 1523.
(105) Bally, M.; Halter, M.; Voros, J.; Grandhin, H. M. *Surf. Interface Anal.* **2006**, *38*, 1442.
(106) Peera, S. G.; Lee, T. G.; Sahu, A. K. *Sustain. Energy Fuels* **2019**, *3*, 1866.
(107) Axet, M. R.; Philippot, K. *Chem. Rev.* **2020**, *120*, 1085.
(108) Han, Y.; Wang, Y. L.; Ma, T. Z.; Li, W.; Zhang, J. L.; Zhang, M. H. *Front. Chem. Sci. Eng.* **2020**, *14*, 689.

(109) Chen, C. Y.; Song, T. X.; Shang, H. Y.; Liu, Q. Y.; Yuan, M. Y.; Wang, C.; Du, Y. K. *Int. J. Hydrogen Energy* **2020**, *45*, 26920.
(110) Delley, B. *J. Chem. Phys.* **1990**, *92*, 508.
(111) Delley, B. *J. Phys. Chem.* **1996**, *100*, 6107.
(112) Delley, B. *J. Chem. Phys.* **2000**, *113*, 7756.
(113) Perdew, J. P.; Burke, K.; Ernzerhof, M. *Phys. Rev. Lett.* **1996**, *77*, 3865.
(114) Perdew, J. P.; Burke, K.; Ernzerhof, M. *Phys. Rev. Lett.* **1997**, *78*, 1396.
(115) Halgren, T. A.; Lipscomb, W. N. *Chem. Phys. Lett.* **1977**, *49*, 225.
(116) Wert, C.; Zener, C. *Phys. Rev.* **1949**, *76*, 1169.
(117) Jonsson, H. *Annu. Rev. Phys. Chem.* **2000**, *51*, 623.
(118) Wang, L.; Williams, J. I.; Lin, T.; Zhongc, C.-J. *Catal. Today* **2011**, *165*, 150.
(119) Wang, L.; Kalyanaraman, C.; McCoy, A. B. *J. Chem. Phys.* **1999**, *110*, 11221.
(120) Billing, G. D.; Wang, L. *J. Phys. Chem.* **1992**, *96*, 2572.
(121) Lambie, S.; Steenbergen, K. G.; Gaston, N.; Paulus, B. *Phys. Chem. Chem. Phys.* **2022**, *24*, 98.
(122) Clary, D. C.; Wang, L. *J. Chem. Soc., Faraday Trans.* **1997**, *93*, 2763.
(123) Sarma, B. B.; Maurer, F.; Doronkin, D. E.; Grunwaldt, J.-D. *Chem. Rev.* **2023**, *123*, 379.
(124) Zhu, C. Z.; Fu, S. F.; Shi, Q. R.; Du, D.; Lin, Y. H. *Angew. Chem. Int. Ed.* **2017**, *56*, 13944.
(125) Yuan, B.; Zhuang, J.; Kirmess, K. M.; Bridgmohan, C. N.; Whalley, A. C.; Wang, L.; Plunkett, K. N. *J. Org. Chem.* **2016**, *81*, 8312.
(126) Bheemireddy, S. R.; Ubaldo, P. C.; Finke, A. D.; Wang, L.; Plunkett, K. N. *J. Mater. Chem. C* **2016**, *4*, 3963.
(127) Spivey, K.; Williams, J. I.; Wang, L. *Chem. Phys. Lett.* **2006**, *432*, 163.
(128) Lu, L.; Zou, S.; Fang, B. *ACS Catal.* **2021**, *11*, 6020.
(129) Liu, M.; Zhang, R.; Chen, W. *Chem. Rev.* **2014**, *114*, 5117.
(130) Li, X.; Yang, X.; Zhang, J.; Huang, Y.; Liu, B. *ACS Catal.* **2019**, *9*, 2521.
(131) Wu, C.; Wang, L.; Xiao, Z.; Li, G.; Wang, L. *Phys. Chem. Chem. Phys.* **2020**, *22*, 724.
(132) Wu, R.; Wiegand, K. R.; Ge, L.; Wang, L. *J. Phys. Chem. C* **2021**, *125*, 14275.
(133) Wu, C.; Xiao, Z.; Wang, L.; Li, G.; Zhang, X.; Wang, L. *Catal. Sci. Technol.* **2021**, *11*, 1965.
(134) Wu, C.; Wang, L.; Xiao, Z.; Li, G.; Wang, L. *Chem. Phys. Lett.* **2020**, *746*, 137229.

Table 1.The information of reactants ethanol, ethoxy, acetaldehyde adsorption, acetyl and ethoxy, two hydrogen atoms coadsorption, ethyl acetate, hydrogen adsorption on Cu_n (n= 1, 2, 13) clusters: adsorption energy (ΔE_{ads}), bond distances between Cu and the nearest O (d_{Cu-O}), bond distances between Cu and the nearest C (d_{Cu-C}), and bond distances between Cu and the nearest H (d_{Cu-H}).

Species	E_{ads}(eV)	d_{Cu-O}(Å)	d_{Cu-C}(Å)	d_{Cu-H}(Å)
CH_3CH_2OH-Cu_1 (IS1)	0.26	2.228	3.164	2.604
CH_3CH_2O-Cu_1 (IS2)	2.45	1.802	2.786	3.028
CH_3CHO-Cu_1 (IS3)	0.25	2.213	2.067	2.480
CH_3CO -Cu_1 -OCH_2CH_3 (IS4)	4.48	1.818	1.908	-----
H-Cu_1-H (IS5)	4.24	-----	-----	1.526
$CH_3COOCH_2CH_3$-Cu_1 (FS4)	0.16	2.797	3.588	-----
H_2-Cu_1 (FS5)	0.07	-----	-----	2.383
CH_3CH_2OH-Cu_2 (IS1)	0.62	2.086	3.056	2.557
CH_3CH_2O-Cu_2 (IS2)	1.76	1.818	2.742	2.641
CH_3CHO-Cu_2 (IS3)	0.64	1.984	2.127	2.603
CH_3CO -Cu_2 -OCH_2CH_3 (IS4)	4.23	1.807	1.980	-----
H-Cu_2-H (IS5)	4.66	-----	-----	1.528
$CH_3COOCH_2CH_3$-Cu_2 (FS4)	0.47	2.148	3.097	-----
H_2-Cu_2 (FS5)	0.26	-----	-----	1.757
CH_3CH_2OH-Cu_{13} (IS1)	0.52	2.135	3.145	2.588
CH_3CH_2O-Cu_{13} (IS2)	2.17	1.880	2.789	2.065
CH_3CHO-Cu_{13} (IS3)	0.23	3.348	2.614	1.917
CH_3CO -Cu_{13} -OCH_2CH_3 (IS4)	3.39	1.963	2.092	-----
H-Cu_{13}-H (IS5)	4.81	-----	-----	1.662
$CH_3COOCH_2CH_3$-Cu_{13} (FS4)	0.36	2.191	-----	-----
H_2-Cu_{13} (FS5)	0.21	-----	-----	1.778

Table 2.HOMO-LUMO gap value of the systems before and after the species adsorbed on the Cu clusters.

Species	HOMO (eV)	LUMO (eV)	HOMO-LUMO gap (eV)	E_{ad} （eV）
Cu_1	-4.61	-3.63	0.98	----
Cu_2	-4.54	-2.73	1.81	----
Cu_{13}	-3.64	-3.40	0.24	----
IS(CH_3CH_2OH-Cu_1)	-3.21	-2.34	0.87	0.26
IS(CH_3CH_2OH-Cu_2)	-3.67	-1.37	2.3	0.62
IS(CH_3CH_2OH-Cu_{13})	-3.35	-3.11	0.24	0.52
IS(CH_3CH_2O-Cu_1)	-4.82	-3.34	1.48	2.45
IS(CH_3CH_2O-Cu_2)	-5.14	-4.59	0.54	1.76
IS(CH_3CH_2O-Cu_{13})	-4.17	-3.65	0.52	2.17
IS(CH_3CHO-Cu_1)	-4.16	-3.29	0.87	0.25
IS(CH_3CHO-Cu_2)	-4.49	-2.96	1.53	0.64
IS(CH_3CHO-Cu_{13})	-3.85	-3.62	0.23	0.23
IS(CH_3CO-Cu_1-OCH_2CH_3)	-5.16	-4.5	0.65	4.48
IS(CH_3CO-Cu_2-OCH_2CH_3)	-5.11	-3.56	1.55	4.23
IS(CH_3CO-Cu_{13}-OCH_2CH_3)	-4.00	-3.85	0.15	3.39
IS(H-Cu_1-H)	-5.77	-4.7	1.07	4.24
IS(H-Cu_2-H)	-4.96	-3.63	1.33	4.66
IS(H-Cu_{13}-H)	-3.9	-3.67	0.23	4.81

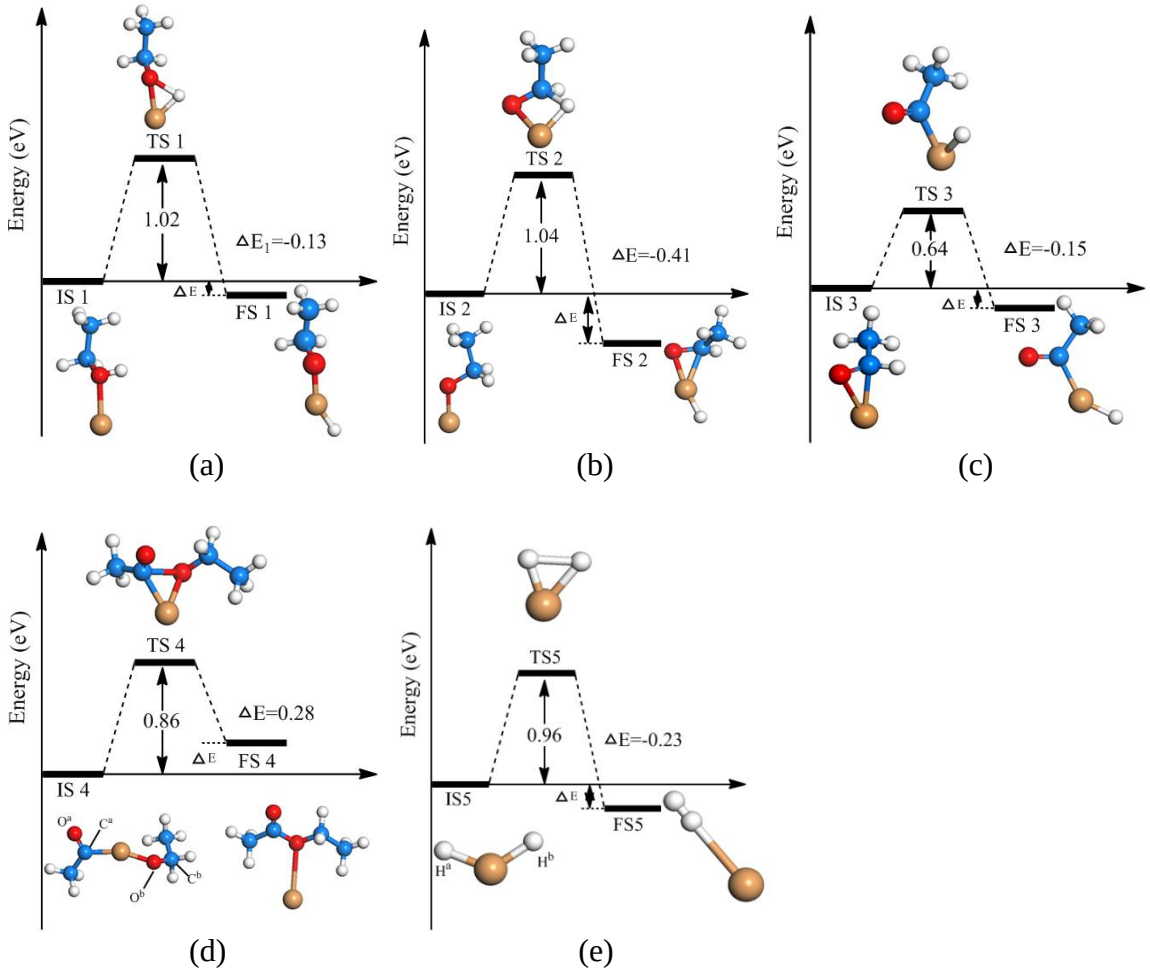

Figure 1.Reaction pathways of ethanol dehydrogenation to ethoxy (a), ethoxy dehydrogenation to acetaldehyde (b), acetaldehyde dehydrogenation to acetyl (c), formation of ethyl acetate from ethoxy and acetyl (d) and hydrogen formation on single Cu atom. Grey spheres = C, white spheres = H, red spheres = O, yellow spheres = Cu.

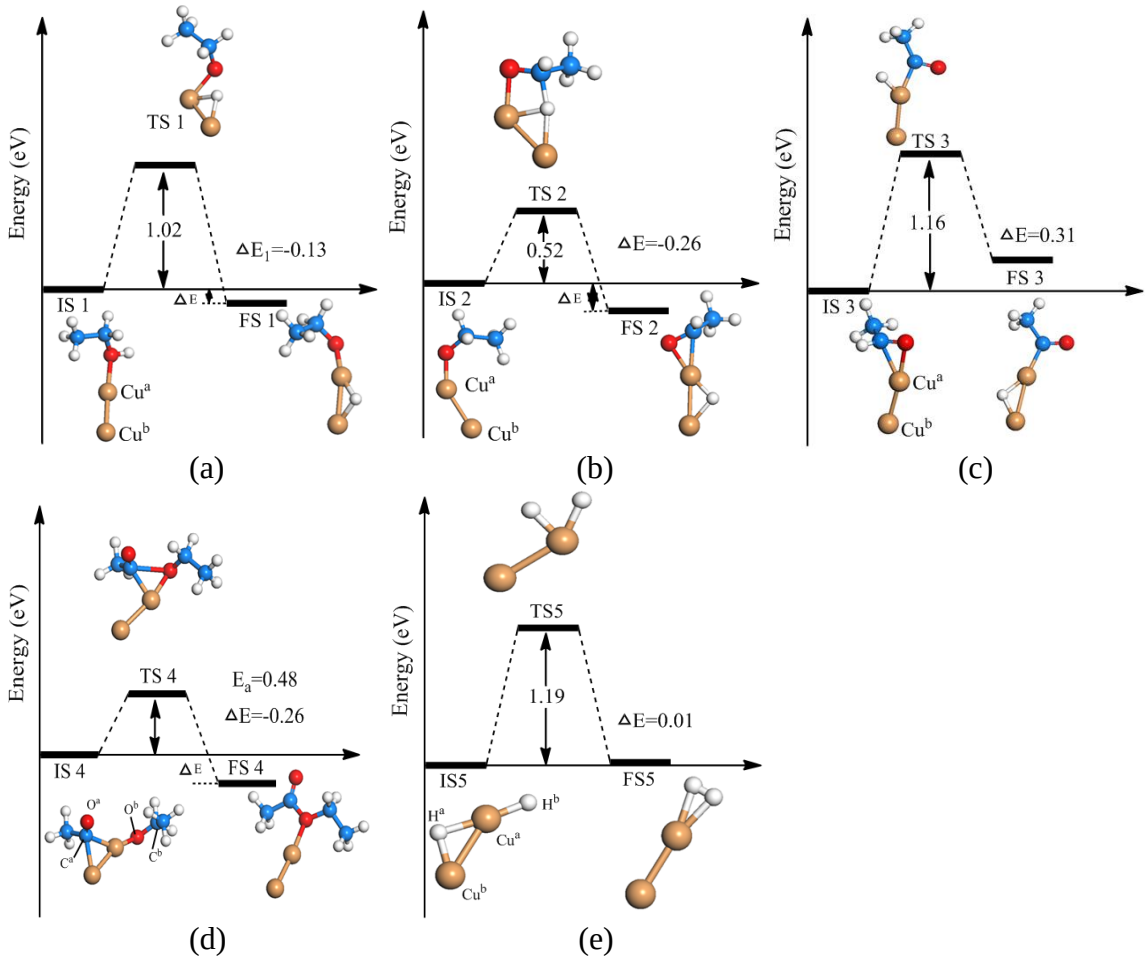

Figure 2.Reaction pathways of ethanol dehydrogenation to ethoxy (a), ethoxy dehydrogenation to acetaldehyde (b), acetaldehyde dehydrogenation to acetyl (c), formation of ethyl acetate from ethoxy and acetyl (d), and hydrogen formation on Cu_2 cluster. Grey spheres = C, white spheres = H, red spheres = O, yellow spheres = Cu.

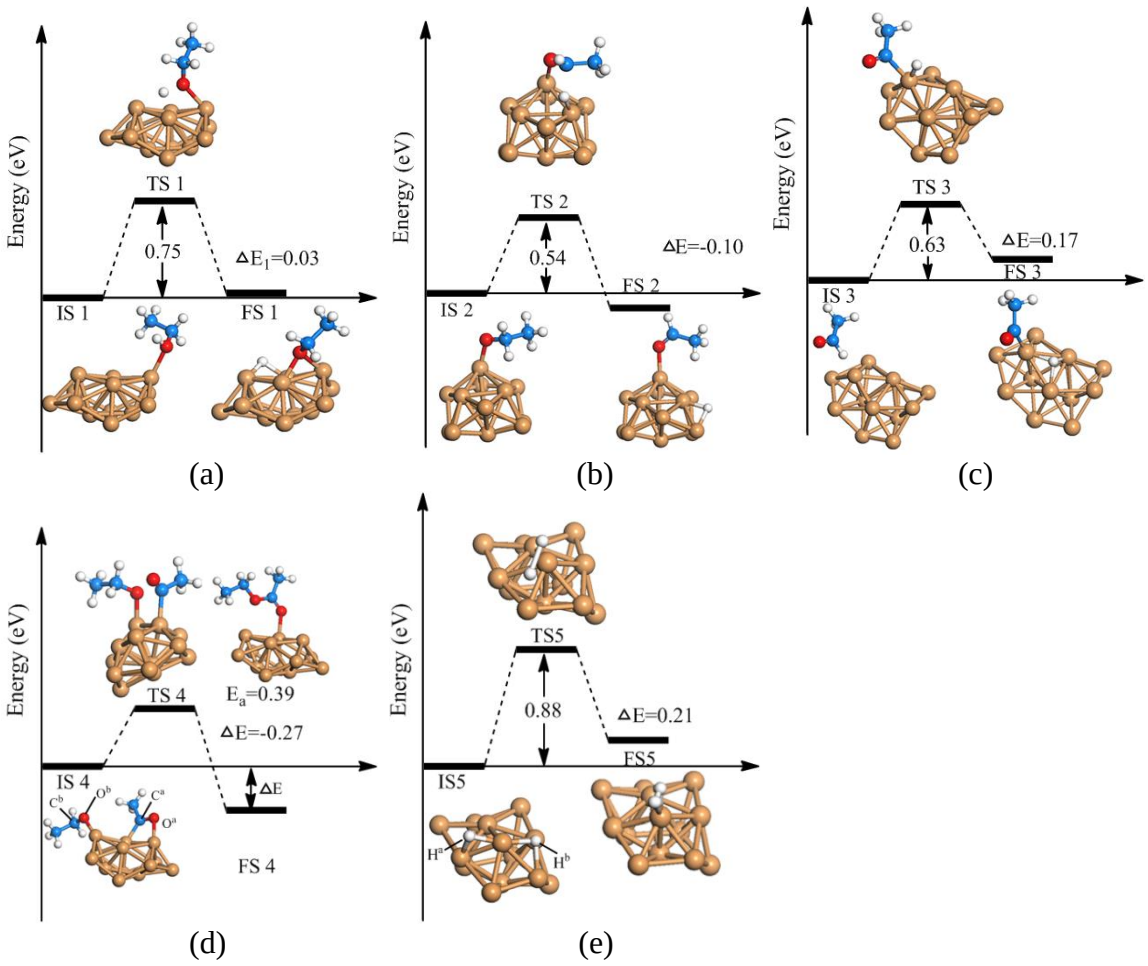

Figure 3.Reaction pathways of ethanol dehydrogenation to ethoxy (a), ethoxy dehydrogenation to acetaldehyde (b), acetaldehyde dehydrogenation to acetyl (c), formation of ethyl acetate from ethoxy and acetyl (d), and hydrogen formation on Cu_{13} cluster. Grey spheres = C, white spheres = H, red spheres = O, yellow spheres = Cu.

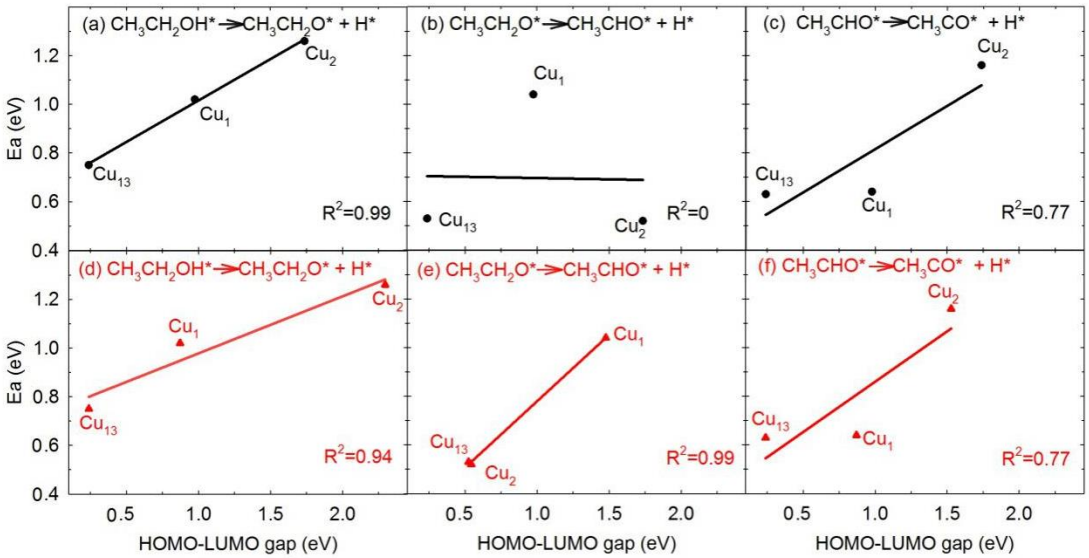

Figure 4.Variation of the catalytic dehydrogenation reaction barriers as a function of HOMO-LUMO gap; the black line (a), (b) and (c) corresponding to the relationship between the HOMO-LUMO gap of Cu clusters and the reaction barriers, the red line (e), (d) and (f) corresponding to the relationship between the reaction barriers and the HOMO-LUMO gap of the system after species adsorbed on Cu clusters.

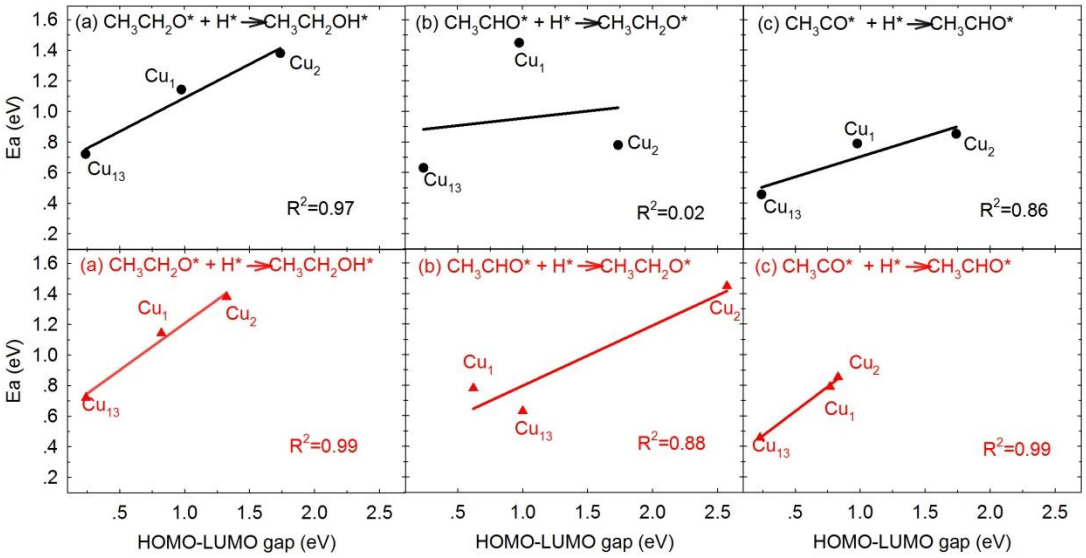

Figure 5. Variation of the catalytic hydrogenation reaction barriers as a function of HOMO-LUMO gap; the black and red line have the same meaning as in Figure 3.

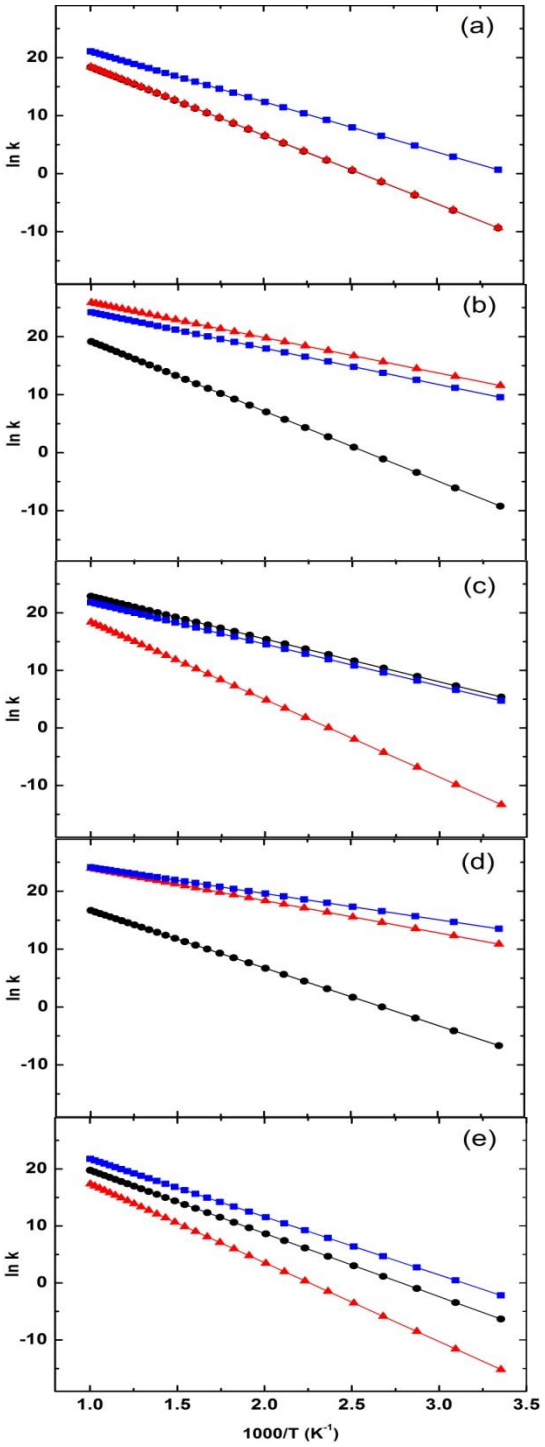

Figure 6. A comparison of the forward reaction constant *k* for each elementary reaction on different size Cu_n (n=1, 2, 13) clusters. The black circles represent the Cu_1, the red triangles represent the Cu_2, and the blue diamond represent the Cu_{13}.

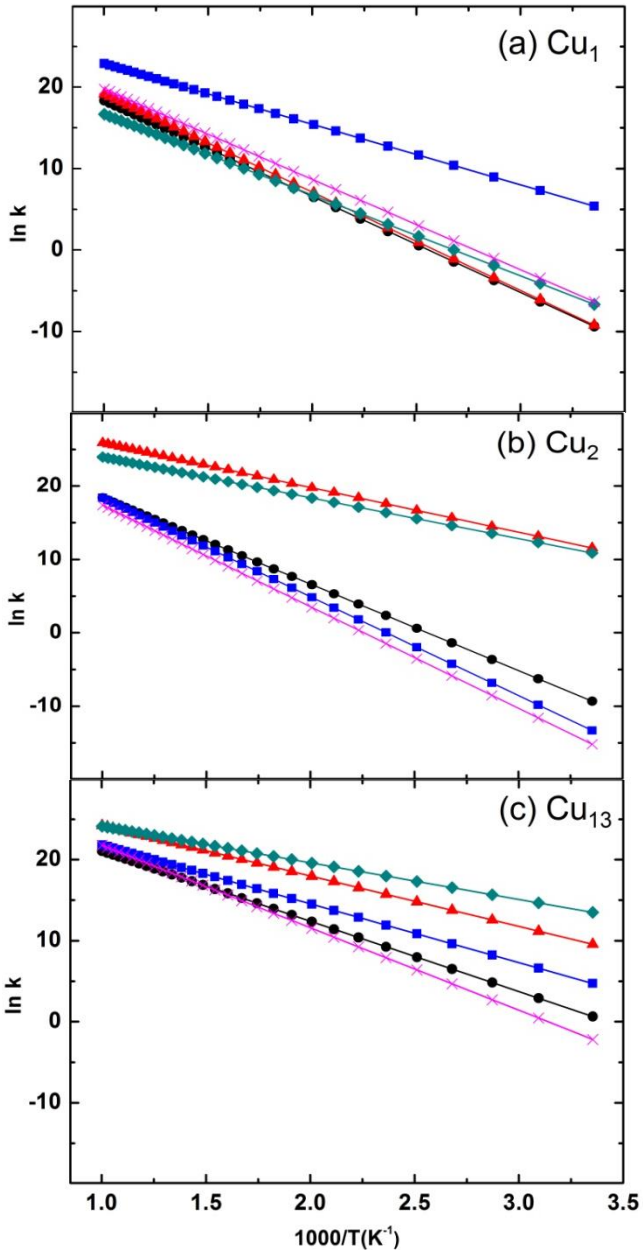

Figure 7.Temperature-dependent curves for the rate constant of each elementary step; the black line represents the elementary step for ethanol to ethoxy, the red line represents the elementary step for ethoxy to acetaldehyde, the blue line represents the elementary step for acetaldehyde to acetyl, the green line represents the elementary step for the formation of ethyl acetate from ethoxy and acetyl, the pink line represents the elementary step for the formation of hydrogen.

Graphical TOC Entry